MODELING THE ORIGINS OF COMPLEX ORGANIC MOLECULES

DURING SOLAR-TYPE STAR FORMATION

Brielle Shope (author), Robin T. Garrod (advisor)

Department of Chemistry, University of Virginia, Charlottesville, VA 22904

Abstract: Life as we know it originated on Earth in the form of molecules. Where did these molecules come from? Were they formed on Earth or delivered to Earth from an earlier time? Recent findings indicate that biologically relevant molecules came from farther back in the solar system timeline than originally thought - all the way back to the very earliest stages of star formation. Before the Earth and Sun existed, our solar system existed as a cloud of gas and dust. The dense cloud collapsed to form a new star with a surrounding disk of material that eventually formed into planets. The objective of this project is to computationally model the evolution of chemistry over the Solar System history. Until now, no theoretical models have been able to provide a physically and chemically accurate picture of the star-formation process. The results of my model are compared to James Webb Space Telescope observations of molecules in solar-type star-forming regions. My research contributes to the scientific community a more complete story of the chemical content over the history of the Solar System.

Introduction

Recent findings indicate that many complex – and potentially pre-biotic – molecules present in the young solar system may have their origins in the very earliest stages of star formation.[1] Observations of low-mass star-forming cores called "hot corinos" provide us with insight into the chemical conditions that were present when the young Sun was forming, prior to the formation of the protoplanetary disk (the Class II Young Stellar Object or YSO stage) that eventually yielded planets and comets. Hot corinos, which can be Class 0 – I YSOs (Figure 1), are particularly noteworthy because of the great diversity and complexity of organic molecules that are detected there, in the gas phase, through microwave molecular emission spectroscopy using instruments such as the Atacama Large Millimeter Array (ALMA). The largest of these molecules, known as COMs (complex organic molecules), include species such as methanol (CH_3OH) and glycolaldehyde ($HCOCH_2OH$)[2], while propanol (C_3H_7OH)[3,4] and urea (NH_2CONH_2)[5] have been detected in hot cores, the high-mass equivalents of hot corinos. These complex molecules are typically understood to be formed on cold dust-grain surfaces, forming ices that later desorb during the "hot" stage (T > ~100 K) when the protostar warms the surrounding dust and gas.[6] ALMA has provided much evidence concerning COMs in the hot regions,[7] and it is hoped that JWST will soon provide further information about the presence and spatial distribution of solid-phase COMs on the icy grains in the colder, outer envelope. However, until recently, no astrochemical models have been able to provide a physically and chemically accurate picture of complex organic molecule production during the low-mass star formation process.

Much evidence now points to many COMs being formed in the very first stages of star formation (Figure 1), during the pre-stellar stage before a protostar is even formed[8-12], when dust and gas temperatures are <10 K. However, further chemistry must occur after the protostar has formed within its surrounding envelope (Class 0) and as the envelope accretes substantially onto the protostar and nascent disk (Class I). As parts of the envelope
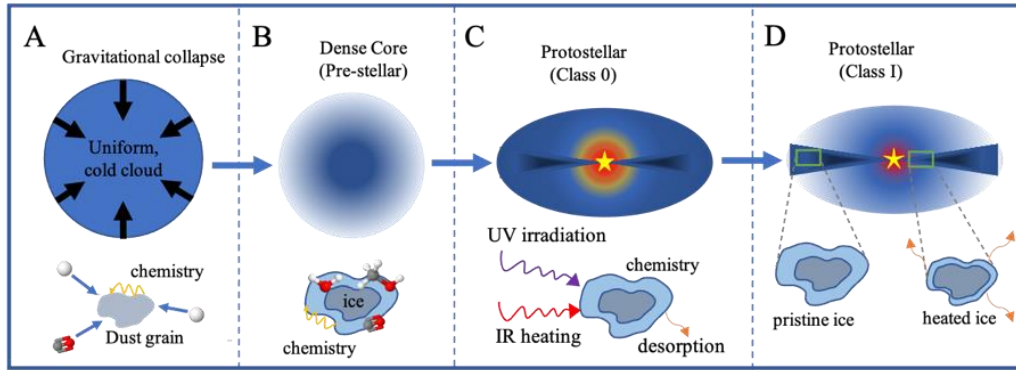
Figure 1: Young Stellar Object (YSO) stages and corresponding grain-ice chemistry. From the left, a uniform cloud collapses into a dense pre-stellar core. During this stage, hydrogen and other atoms and simple molecules accrete onto the dust-grain surface and form an icy mantle, through surface chemistry. As the protostar accretes material from the surrounding envelope (Class 0), UV-induced chemistry occurs on grain surfaces and molecules in the warm inner regions start to desorb. In Class I, much of the envelope mass has been accreted onto the protostar and the disk has grown. Ices near the protostar completely desorb into the gas phase, while grains in the outer envelope stay intact.

and disk reach high temperatures (>100K), grain-surface species nearest to the protostar will desorb into the gas-phase and ultimately be destroyed, but molecules on the dust grains in the cold outer envelope should survive by avoiding the protostar's harsh environment.[1] This would suggest that the latter could constitute the inheritance that is passed on to comets.

To test these ideas, it is necessary to have astrochemical models that are (i) capable of simulating COM chemistry both on the dust grains and in the gas, and (ii) physical/dynamical models to combine with the chemical models, so that the motions of gas and dust, beginning in the pre-stellar stage and culminating in the formation of a disk, can be properly coupled to the chemical evolution. Only then can a full spatial picture of COM chemistry be built up.

In this project, we use the astrochemical model MAGICKAL (Model for Astrophysical Gas and Ice Chemical Kinetics and Layering), which is a three-phase chemical kinetics model (gas, grain-surface, and mantle-ice chemistry[13]). Due to its detailed COM chemical network and ice kinetics treatments, it is the most advanced model of grain-surface COM chemistry in use in the field.[14] This model has many capabilities including the ability to trace ice and gas abundances of Young Stellar Objects (YSOs) from Class 0 through I. Coupled with a multidimensional hydrodynamics model with solar-type conditions, it creates the most chemically and physically accurate picture of COM chemistry

during the early stages of our Solar System formation.

Methods

Two state-of-the-art models are used to carry out the project (MAGICKAL for the chemistry and ATHENA++ for dynamics). The dynamical models are applied to the pre-stellar collapse through Class I (stages B – D in Figure 1), with Lagrangian particle trajectories calculated in post-processing. The dynamical models work in an Eulerian frame, while the chemical models require a Lagrangian frame of reference, requiring that the chemical models be run in post processing. Trajectories for the earlier collapse from a uniform cloud to a pre-stellar core are calculated analytically (stage A in Figure 1). For each of the 3413 tracer particles, the chemistry of a parcel of gas is simulated, with position and physical conditions evolving over time. The chemistry is thus traced continuously from a uniform cloud all the way to a Class I YSO.

Radiation Hydrodynamics Models

The dynamical treatment uses a private version of the publicly available ATHENA++ v20.0 code[15,16] that includes radiation, self-gravity and dust modules. These 2-D simulations use a fixed spherical-polar grid assuming ϕ displacement symmetry. The protostellar collapse starts from a pseudo Bonnor-Ebert (B-E sphere), with an initial solid-body rotation and viscosity assigned. Matter that passes inside the central (10 au) boundary is
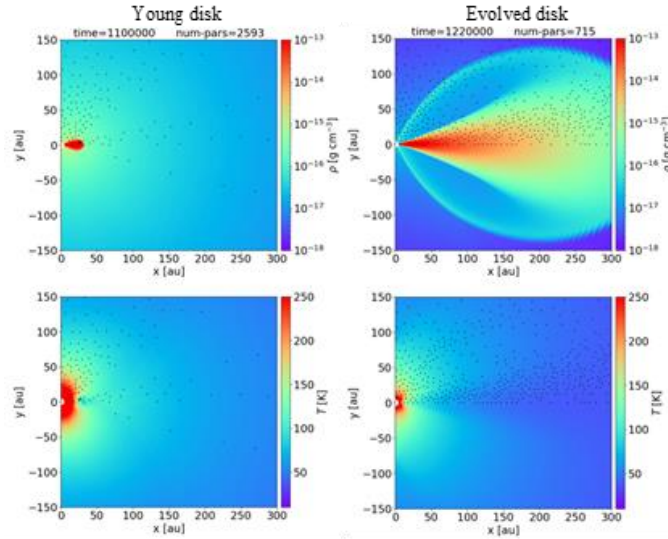
Figure 2 Sample data of axisymmetric (2-D) radiation hydrodynamics (RHD)/chemical models. The dynamical models produce trajectories (black dots) with varying physical conditions. Top panels show hydrogen number density distribution and bottom panels show the temperature distribution throughout from an initial Class 0 state (left) to a later Class I state (right). The evolution from stages B – D (see Fig. 1) lasts 1.22 Myr and ends when a disk of radius ~300 au has formed.

added to the mass of the protostar. As the mass of the protostar grows (from zero), it irradiates the surrounding dust with IR, raising the temperature; the mass-luminosity relations of Hosokawa & Omukai (2009)[17] are used.

Based on the RHD model results, which are already complete, Lagrangian tracer particle trajectories are calculated in post-processing. Tracers are positioned to ensure good spatial sampling at 21 evenly-spaced points in time, requiring 3413 particles. Figure 2 shows the gas density and temperature results of the RHD model, along with preliminary tracer positions. The tracers provide gas density, dust/gas temperature, visual extinction, and position information from the RHD models that are fed to the chemical models. Due to the symmetry, tracer particles are only distributed through the upper quadrant of the simulation space. The chosen tracer particles are then evolved backward to approximate the initial collapse to a pre-stellar core.

Chemical models

The three-phase (gas/surface/ice-mantle) gas-grain chemical kinetics code MAGICKAL[13] includes

common COMs like methanol and methyl formate, but also glycine[13] and simple sugars. With the largest chemical network of ~27,000 reactions and processes, it has perhaps the most advanced network for COMs, and is unique in having a full, self-consistent framework for the treatment of both diffusive and non-diffusive grain-surface and bulk-ice chemical reactions, using the kinetics framework set up by Jin & Garrod (2020)[17] and Garrod et al. (2022)[14].

Early chemical models relied on gas-phase ion-molecule chemistry to produce a range of detected COMs.[18–20] In these models, thermal desorption of simple ice species from the grains drove gas-phase production. However, measurements of certain reaction rates and product branching ratios[21,22] indicate that gas-phase ion-molecule chemistry alone is likely not capable of explaining the presence of all detected COMs, in particular the ubiquitous methyl formate ($HCOOCH_3$). Therefore, in response, most recent chemical models have incorporated some type of active dust-grain chemistry that allows simple molecules to be converted into COMs on the grain surfaces during the warm-up stage, prior to desorption.[13,23-26] Although these considerations are successful in

broadly reproducing observed gas-phase molecular abundances, the recent detection of COMs including methyl formate, dimethyl ether (CH3OCH3) and acetaldehyde (CH3CHO) in cold, pre-stellar cores,[16,19] in quantities as high as ~10−10n[H2] (i.e. ~1% of "hot" values), suggests the need for models to simulate COM production at low temperatures.

Production of COMs on grains in the early pre-stellar stage when grain temperatures are below 10K requires non-diffusive mechanisms. The Jin & Garrod (2020)[25] and Garrod et al. (2022)[21] frameworks consider non-diffusive mechanisms including "three-body" reactions, in which an initiating surface reaction leads to an immediate follow-on reaction of the product with some other nearby species, without mediation by thermal diffusion. This framework was also applied to photodissociation-driven chemistry, thus avoiding any requirement for the thermal diffusion of radicals in the bulk ices, removing much of the temperature dependence, and shifting the onset of photo-production of COMs to low temperatures, in line with laboratory evidence.[34]

MAGICKAL is currently the only astrochemical model that includes a full implementation of diffusive and non-diffusive chemistry. This makes it ideally suited to the study of COM chemistry from the pre-stellar through Classes 0 and I stages of protostellar YSO evolution, which, based on laboratory and observational evidence, may be strongly influenced by the formation of COMs on cold grain surfaces. Combined with dynamics, the resulting models are the first to simulate the unbroken chain of chemistry from a molecular cloud to a protostar and disk.

These model results allow proper comparisons to JWST and ALMA[2,10,16–19] data, by integrating column densities through the source and mapping them. By modeling the gas and ice chemistry over time, we obtain snapshots of the spatial and temporal distribution of COMs and their abundance in the growing disk.

Column Density and Excitation Temperature Calculations

Gas-phase column densitites and excitation temperatures are calculated with use of an in-house

RADMC-3D treatment. RADMC-3D is a package that allows users to conduct radiative transfer calculations to generate 2D synthetic images of their data in order to compare to observations. In addition to these synthetic images, this work makes use of further treatment as developed by Bonfand 2024 (in prep) to derive gas-phase column densities and excitation temperatures. Refer to Bonfand 2024 (in prep) for details pertaining to this treatment.

This RADMC-3D treatment allows the user to account for dust emission and radiative transfer in the calculations of excitation temperatures and column densities. This treatment is used for the gas-phase column densities reported in this paper. All ice column densities are calculated by integrating the abundances over the line of sight.

Results & Discussion

Stage 1 COM Abundances Over Time

The MAGICKAL model is split into two stages. The first stage is the collapse stage, as depicted in letters A and B in Figure 1. The collapse is assumed uniform in the polar direction but allowed to vary in the radial direction.

In this stage, due to cold temperatures (<10K) COMs are formed on the grain through non-diffusive mechanisms. In Figure 3, the abundances of simple species and of COMs at the beginning of Stage 1 are shown over the entirety of time of Stage 1. The abundances are constant radially at the beginning and as time progresses (see the bottom four plots of Figure 3), the abundance of these species changes spatially.

At the end of Stage 1, most of the species in the gas-phase show a rampant drop-off due to freeze out. Note that there are a few species in which the abundances peak a various places radially within the disk. When considering gas-phase methanol, its abundance does peak in the outer rim as seen in observations. Formaldehyde and acetaldehyde also show peaks at various radii. As the density increases, there is more production of these species. However, as the model reaches the outer rims, the external radiation increases, leading to less production. As one reaches radii closest to the forming star, the lower the visual extinction,

meaning more photodissociation. Once also sees that with methyl formate, there is a peak towards the outer rim. At this radial position, more solid species survive. The rate of hydrogen species being ripped off methyl formate drops, leading to a higher abundance.
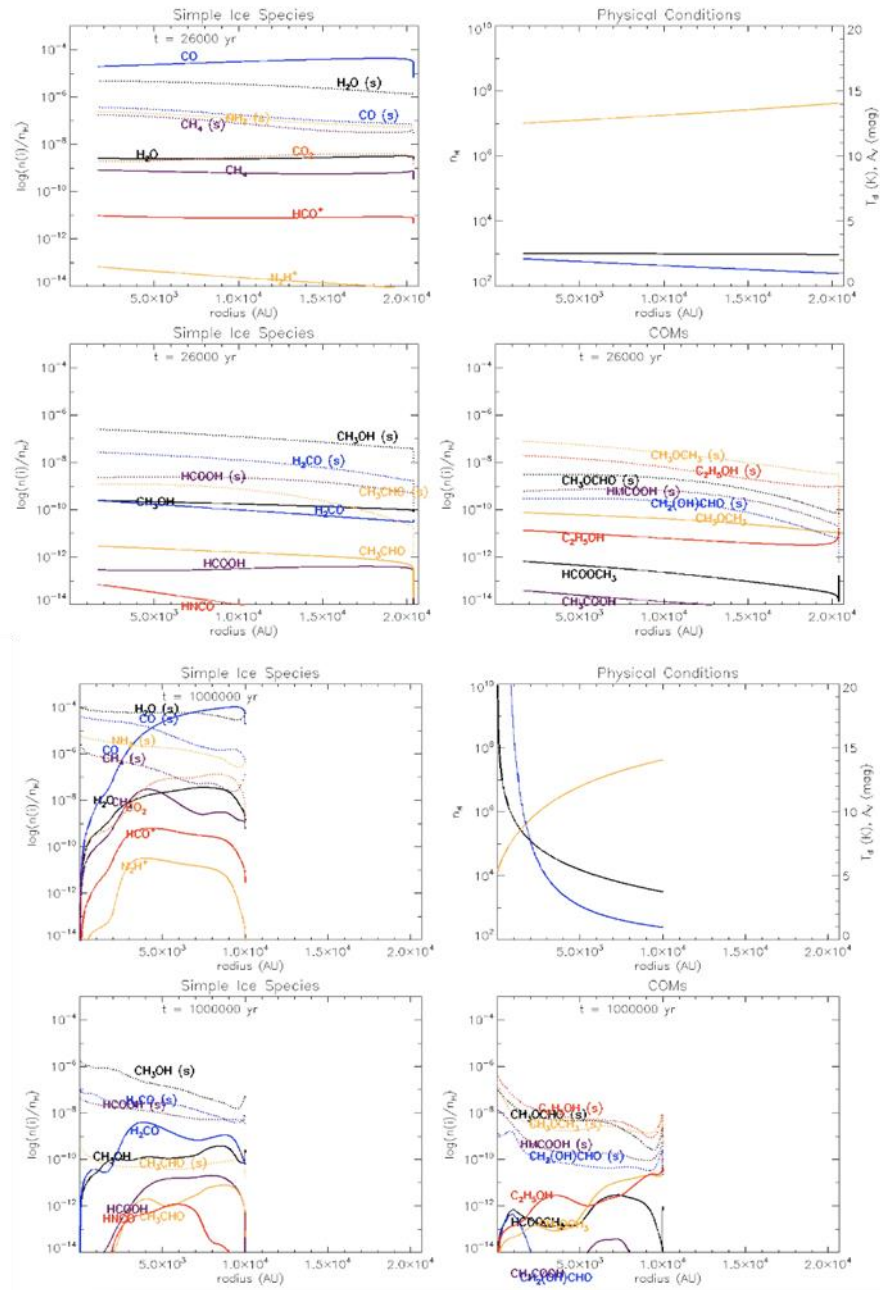

Figure 3 Simple Ice Species and COM abundances over time during Stage 1 of the MAGICKAL model for both the beginning of the Stage 1 when a uniform cold cloud and end time of Stage 1 after the collapse is done. Dotted lines are grain species and solid lines are gas-phase. In the physical conditions plot, the orange is the visual extinction, the black is the hydrogen number density, and the blue is the dust temperature.

Table 1. Absolute ice column densities and column densities relative to H_2O for stage 1 of the MAGICKAL model. Three time points are selected to compare to McClure et al 2023 and Boogert 2015 observational values.

	Model						Literature		
	750 ×10³ yrs		950 ×10³ yrs		1×10⁶ yrs		NIR38	J110621	BG Stars
Species	N_{ice} (×10¹⁸ cm⁻²)	X_{H_2O}(%)	N_{ice} (×10¹⁸ cm⁻²)	X_{H_2O}(%)	N_{ice} (×10¹⁸ cm⁻²)	X_{H_2O}(%)	N_{ice} (×10¹⁸ cm⁻²) (McClure)	N_{ice} (×10¹⁸ cm⁻²) (McClure)	X_{H_2O}(%) (Boogert)
H_2O	0.54	100	10.13	100	562	100	6.88	13.38	100
CO	0.17	31	5.47	54	315	56	2.96	3.68	9-67
CO_2	0.44	82	8.25	81	402	71	1.38	1.74	14-43
CH_3OH	0.007	1	0.23	2	16.7	3	0.41	0.45	(<1)-12
NH_3	0.04	7	0.75	7	44.0	8	0.30	0.66	<7
CH_4	0.004	0.7	0.072	0.7	3.96	0.7	0.18	0.25	<3

Column Densities

The column densities of selected species are presented in Table 1. Three times are selected to compare to literature values of background stars (McClure et al 2023 and Boogert 2015). The total time of Stage 1 is set to one million years. The final value is given as well as a time slightly before the final end mark in order to give insight on how quickly the column densities increase toward the end of stage 1. At the time of 950 ×10³ yrs, the column densities more closely match those in the literature. CO_2 is overproduced in our models as compared to literature data. The source NIR38 has a visual extinction of 60 mag and the source J110621 has a visual extinction of 95 mag. At the end of the Stage 1 model, the visual extinction has reached 3000mag.

Stage 2 Abundance Maps

In Stage 2, the warm-up phase, the model tracks the abundances of species spatially as well. Polar symmetry is no longer assumed as there is now a formation of a disk. In Figure 4, the abundances of H_2O, CO, and CH_3OH change spatially with time. The left three panels are a young disk where the abundances are centrally located around the protostar. In the three panels on the right, the system has evolved to a protostellar disk. In the young disk panel for methanol, one can see the similar effect of a peak of methanol abundance towards the outer rim just as seen in Figure 3 and in observations.

Future Steps

Now that Stage 1 and Stage 2 models are all complete, one piece of analysis left to do is to compare the ice column densities of stage 1 and stage 2. However, in stage 2, the column densities are not assumed to have polar symmetry due to the formation of the disk. Depending on the angle at which one views the disk, whether edge-on, face-on, or somewhere in between, the column densities vary.
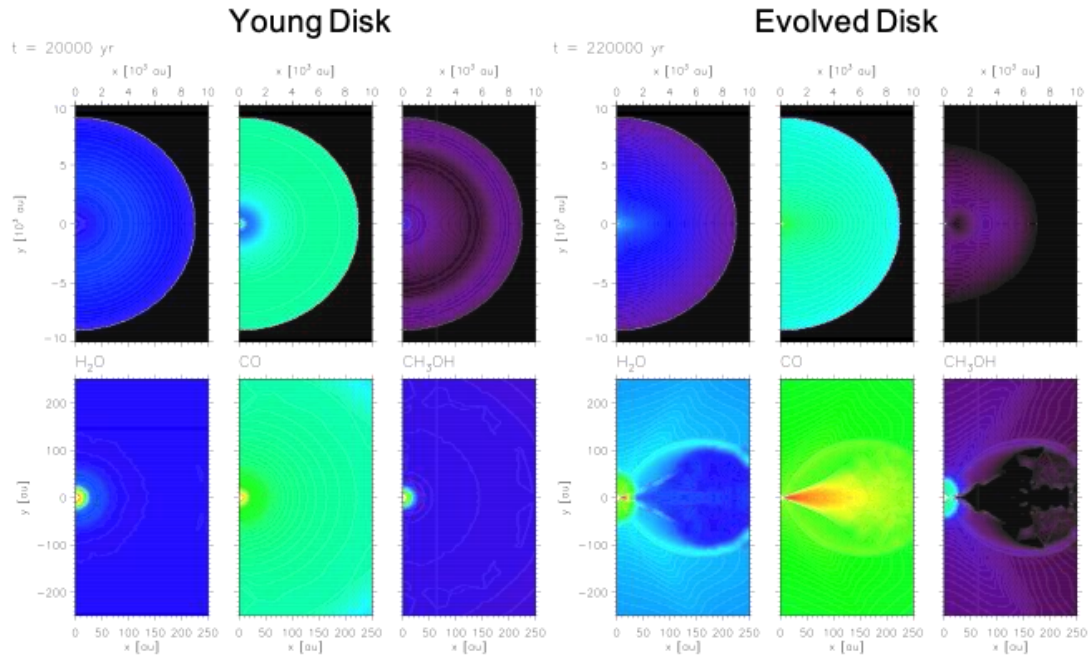
Young Disk　　　Evolved Disk

Figure 4 Absolute Abundance Maps of H_2O, CO, and CH_3OH.

In addition to ice column densities, gas-phase column densities need to be calculated for a variety of species. These will be calculated via the RADMC-3D treatment as discussed earlier. These calculations will also be calculated for various inclination angles. We will compare between observational data of face-on and edge-on sources such as IRAS 16293b and IRAS 16293a, respectively.

Once all this data is collected, we will make final conclusions as to the dependencies of various species abundances – simple and COMs – on the temporal, spatial, and inclination parameters.

References

(1)　Drozdovskaya, M. N.; Van Dishoeck, E. F.; Rubin, M.; Jørgensen, J. K.; Altwegg, K. Ingredients for Solar-like Systems: Protostar IRAS 16293-2422 B versus Comet 67P/Churyumov–Gerasimenko. *Mon. Not. R. Astron. Soc.* **2019**, *490* (1), 50–79.

(2)　Jørgensen, J. K.; Favre, C.; Bisschop, S. E.; Bourke, T. L.; van Dishoeck, E. F.; Schmalzl, M. DETECTION OF THE SIMPLEST SUGAR, GLYCOLALDEHYDE, IN A SOLAR-TYPE PROTOSTAR WITH ALMA. *Astrophys. J.* **2012**, *757* (1), L4.

(3)　Belloche, A.; Garrod, R. T.; Zingsheim, O.; Müller, H. S. P.; Menten, K. M. Interstellar Detection and Chemical Modeling of Iso-Propanol and Its Normal Isomer. *A&A* **2022**, *662*.

(4)　Jiménez-Serra, I.; Rodríguez-Almeida, L. F.; Martín-Pintado, J.; Rivilla, V. M.; Melosso, M.; Zeng, S.; Colzi, L.; Kawashima, Y.; Hirota, E.; Puzzarini, C.; et al. Precursors of Fatty Alcohols in the ISM: Discovery of n-Propanol. *A&A* **2022**, *663*.

(5)　Belloche, A.; Garrod, R. T.; Müller, H. S. P.; Menten, K. M.; Medvedev, I.; Thomas, J.; Kisiel, Z. Re-Exploring Molecular Complexity with ALMA (ReMoCA): Interstellar Detection of Urea. *Astron. Astrophys.* **2019**, *628*.

(6)　Herbst, E.; van Dishoeck, E. F. Complex Organic Interstellar Molecules. *Annu. Rev.*

Astron. Astrophys. **2009**, *47* (1), 427–480.

(7) Jørgensen, J. K.; Belloche, A.; Garrod, R. T. Astrochemistry During the Formation of Stars. *Annu. Rev. Astron. Astrophys.* **2020**, *58* (1), 727–778.

(8) Megías, A.; Jiménez-Serra, I.; Martín-Pintado, J.; Vasyunin, A. I.; Spezzano, S.; Caselli, P.; Cosentino, G.; Viti, S. The Complex Organic Molecular Content in the L1517B Starless Core. *Mon. Not. R. Astron. Soc.* **2022**, *519* (2), 1601–1617.

(9) Bacmann, A.; Taquet, V.; Faure, A.; Kahane, C.; Ceccarelli, C. Detection of Complex Organic Molecules in a Prestellar Core: A New Challenge for Astrochemical Models. *Astron. Astrophys.* **2012**, *541*, L12.

(10) Marcelino, N.; Cernicharo, J.; Agúndez, M.; Roueff, E.; Gerin, M.; Martín-Pintado, J.; Mauersberger, R.; Thum, C. Discovery of Interstellar Propylene (CH2CHCH3): Missing Links in Interstellar Gas-Phase Chemistry. *Astrophys. J.* **2007**, *665* (2), L127.

(11) Öberg, K. I.; Bottinelli, S.; Jørgensen, J. K.; van Dishoeck, E. F. A COLD COMPLEX CHEMISTRY TOWARD THE LOW-MASS PROTOSTAR B1-b: EVIDENCE FOR COMPLEX MOLECULE PRODUCTION IN ICES*. *Astrophys. J.* **2010**, *716* (1), 825.

(12) Jiménez-Serra, I.; Vasyunin, A. I.; Caselli, P.; Marcelino, N.; Billot, N.; Viti, S.; Testi, L.; Vastel, C.; Lefloch, B.; Bachiller, R. THE SPATIAL DISTRIBUTION OF COMPLEX ORGANIC MOLECULES IN THE L1544 PRE-STELLAR CORE. *ApJL* **2016**, *830* (1), L6.

(13) Garrod, R. T. A Three-Phase Chemical Model of Hot Cores: The Formation of Glycine. *ApJ* **2013**, *765* (60), 29.

(14) Garrod, R. T.; Jin, M.; Matis, K. A.; Jones, D.; Willis, E. R.; Herbst, E. Formation of Complex Organic Molecules in Hot Molecular Cores through Nondiffusive Grain-Surface and Ice-Mantle Chemistry. *Astrophys. J. Suppl. Ser.* **2022**, *259* (1), 1.

(15) Stone, J. M.; Gardiner, T. A.; Teuben, P.; Hawley, J. F.; Simon, J. B. Athena: A New Code for Astrophysical MHD. *Astrophys. J. Suppl. Ser.* **2008**, *178* (1), 137.

(16) Stone, J. M.; Tomida, K.; White, C. J.; Felker, K. G. The Athena++ Adaptive Mesh Refinement Framework: Design and Magnetohydrodynamic Solvers. *Astrophys. J. Suppl. Ser.* **2020**, *249* (1), 4.

(17) Jin, M.; Garrod, R. T. Formation of Complex Organic Molecules in Cold Interstellar Environments through Nondiffusive Grain-Surface and Ice-Mantle Chemistry. *ApJS* **2020**, *249*, 26.

(18) Millar, T. J.; Herbst, E.; Charnley, S. B. The Formation of Oxygen-Containing Organic Molecules in the Orion Compact Ridge. *ApJ* **1991**, *369*, 147.

(19) Viti, S.; Williams, D. A. Time-Dependent Evaporation of Icy Mantles in Hot Cores. *Mon. Not. R. Astron. Soc.* **1999**, *305* (4), 755–762.

(20) Charnley, S. B.; Kress, M. E.; Tielens, A. G. G. M.; Millar, T. J. Interstellar Alcohols. *ApJ* **1995**, *448*, 232.

(21) Horn, A.; Møllendal, H.; Sekiguchi, O.; Uggerud, E.; Roberts, H.; Herbst, E.; Viggiano, A. A.; Fridgen, T. D. The Gas-Phase Formation of Methyl Formate in Hot Molecular Cores. *Astrophys. J.* **2004**, *611* (1), 605.

(22) Geppert, W. D.; Hamberg, M.; Thomas, R. D.; Österdahl, F.; Hellberg, F.; Zhaunerchyk, V.; Ehlerding, A.; Millar, T. J.; Roberts, H.; Semaniak, J.; et al. Dissociative Recombination of Protonated Methanol. *Faraday Discuss.* **2006**, *133* (0), 177–190.

(23) Gorai, P.; Das, A.; Majumdar, L.; Chakrabarti, S. K.; Sivaraman, B.; Herbst, E. The Possibility of Forming Propargyl Alcohol in the Interstellar Medium. *Mol. Astrophys.* **2017**, *6*, 36–46.

(24) Allen, V.; van der Tak, F. F. S.; Walsh, C. Complex Cyanides as Chemical Clocks in Hot Cores. *A&A* **2018**, *616*.

(25) Majumdar, L.; Loison, J.-C.; Ruaud, M.; Gratier, P.; Wakelam, V.; Coutens, A. Methyl Isocyanate (CH3NCO): An Important Missing Organic in Current Astrochemical Networks. *Mon. Not. R. Astron. Soc. Lett.* **2018**, *473* (1), L59–L63.

(26) Henderson, B. L.; Gudipati, M. S. DIRECT DETECTION OF COMPLEX ORGANIC PRODUCTS IN ULTRAVIOLET (Lyα) AND ELECTRON-IRRADIATED ASTROPHYSICAL AND COMETARY ICE ANALOGS USING TWO-STEP LASER ABLATION AND IONIZATION MASS SPECTROMETRY. *Astrophys. J.* **2015**, *800* (1), 66.